Stability Analysis of Underwater Snake Robot Locomotion Based on Averaging Theory

E. Kelasidi, K. Y. Pettersen and J. T. Gravdahl

Abstract— **This paper presents an averaged model of the velocity dynamics of an underwater snake robot, suited for stability analysis and motion planning purposes for general sinusoidal motion gait patterns. Averaging theory is applied in order to derive a model of the average velocity for a control-oriented model of an underwater snake robot that is influenced by added mass effects (reactive fluid forces) and linear drag forces (resistive fluid forces). Based on this model we show that the average velocity of an underwater snake robot during sinusoidal motion patterns converges exponentially to a steady-state velocity. An explicit analytical relation is given between the steady state velocity and the amplitude, the frequency, the phase shift and the offset of the joint motion for the case of a sinusoidal gait pattern. The results of the paper are general and constitute a powerful tool for achieving faster forward motion by selecting the most appropriate motion pattern and the best combination of the gait parameters. Simulation results are presented both for lateral undulation and eel-like motion.**

I. INTRODUCTION

Inspired by biological swimming creatures, underwater snake robots carry the potential of meeting the growing need for robotic mobility in underwater environments. They thus bring a promising prospective to improve the efficiency and maneuverability of modernday underwater vehicles. Generally, studies of hyper-redundant mechanisms (HRMs), also known as snake robots, have largely restricted themselves to land-based studies [1]. An unambiguous result of all these studies is that the high number of DOFs of snake robots makes them difficult to control, but also gives them the ability to traverse irregular environments. Thus they can surpass the mobility of conventional wheeled, tracked or legged robots [1]. Comparing amphibious snake robots to the traditional ones, the former have the advantage of adaptability to aquatic environments. Underwater snake robots have several promising applications for underwater exploration, monitoring, surveillance and inspection. These mechanisms carry a lot of potential for inspection of subsea oil and gas installations. Also, for the biological community and marine archeology, snake robots that are able to swim smoothly without much noise, and can traverse difficult environments like wrecked ship, are very interesting [2].

J. T. Gravdahl is with the Dept. of Engineering Cybernetics at NTNU, NO-7491 Trondheim, Norway. E-mail: Tommy.Gravdahl@itk.ntnu.no

E. Kelasidi, and K. Y. Pettersen are with the Centre for Autonomous Marine Operations and Systems, Dept. of Engineering Cybernetics at NTNU, NO-7491 Trondheim, Norway. E-mail: {Eleni.Kelasidi,Kristin.Y.Pettersen}@itk.ntnu.no

This work was partly supported by the Research Council of Norway through project no. 205622 and its Centres of Excellence funding scheme, project no. 223254-AMOS

It is well-known that the joint motion of swimming snake robots is periodic [2]. The control-oriented model presented in [3] is specifically designed to capture this motion through capturing the corresponding translational motion during oscillations, and the analysis in this paper will be based on this model. This paper is based on the hypothesis that oscillatory behavior causes some averaged effect that forces the robot to move forward [1], [4]. By converting periodic time-varying systems into time-invariant systems, averaging constitutes a useful tool for simplifying complex systems with periodic and oscillatory behavior [5], [6]. Thus, averaging theory is extensively used for analysis of locomotion of biomimetic systems with oscillatory inputs, and it is applied in several works to study the locomotion of snake or fish robots [1], [4], [7], [8], [5], [9], [10]. For instance, [11] presents second order averaging methods suited for control purposes of underactuated mechanical systems such as fish robots. Averaging-based control methods for the stabilization of driftless underactuated systems by periodic feedback are introduced in [5]. [9] proposes a control-oriented data-driven averaging approach for robotic fish. In [12], based on the dynamic model derived in [9], a target-tracking control problem for a tail-actuated robotic fish is presented.

In this paper, averaging theory will be used to study the dynamics of underwater snake robots during sinusoidal motion. In particular, an averaged model of the velocity dynamics is derived. It is shown that the classical averaging methods can be applied for swimming robots, avoiding to derive the averaged velocity dynamics by scaling the original forcing terms by functions of motion pattern parameters, as it is presented in [9]. This means that the proposed averaged model can be derived using classical averaging, avoiding a control-oriented data-driven averaging approach; a solution presented in [9] for fish robots based on a simulation comparison of the original model and the averaged model obtained through classical averaging.

A similar study was presented in [4] for ground robots. The results in this paper extend this by taking into account the hydrodynamic effects that underwater snake robots experience, i.e. the reactive and resistive fluid forces, including added mass and drag forces. Moreover, while the results in [4] were derived for the particular motion pattern lateral undulation, the results in this paper are derived for any periodic motion pattern. The results in this paper thus extend [4] to amphibious snake robots and general sinusoidal motion patterns, and the results in [4] fall out as a special case when the motion pattern is lateral undulation and when the drag forces are replaced by viscous friction forces. Hence,

this model can be used for stability analysis and control design for a broad class of motion patterns including lateral undulation and eel-like motion.

Based on the averaged model of the velocity dynamics, the stability properties for general sinusoidal motion gait patterns are then investigated. In particular, we show that the averaged velocity of an underwater snake robot during a sinusoidal motion pattern converges exponentially to a steady-state velocity. An analytical expression for calculating this steady-state velocity is presented as a function of the gait pattern parameters. The derived relationship between the gait pattern parameters and the steady-state velocity provides a useful tool for motion planning and parameter tuning of sinusoidal gait patterns for underwater snake robots.

Previous studies for ground snake robots [1], [4] and eel-like robots, where the added mass effects and fluid torques are neglected [7], show that the average forward velocity of the robot during lateral undulation is: 1) proportional to the square of the amplitude of the sinusoidal motion pattern, 2) proportional to the gait frequency and 3) depends also on the weighted sum of the constant phase shift between the joints. In this paper, we show that the average forward velocity of an underwater snake robot, influenced both by added mass and linear drag effects, and under any sinusoidal gait pattern, is: 1) a function of the amplitude of the sinusoidal motion pattern, 2) depends on a linear and a nonlinear term of the gait frequency and 3) depends on the phase shift between the joints. The results of this paper are thus more general and constitute a powerful tool for achieving faster forward motion by selecting the most appropriate motion pattern and the best combination of the gait parameters.

This paper is organized as follows. Section II presents a control-oriented model of an underwater snake robot, followed by controller design in Section III. Section IV develops the averaged velocity dynamics of an underwater snake robot. Section V presents a stability analysis of the averaged velocity dynamics. Simulation results are presented in Section VI, followed by conclusions and suggestions for future research, in Section VII.

II. A CONTROL-ORIENTED MODEL OF AN UNDERWATER SNAKE ROBOT

This section gives a brief description of the control-oriented model of an underwater snake robot moving in a virtual horizontal plane presented in [3], on which the analysis in this paper will be based. The robot is assumed to move in a virtual horizontal plane, fully immersed in water, and has N+2 degrees of freedom. The kinematics and dynamics of the underwater snake robot are given in terms of the mathematical symbols described in Table I and illustrated in Fig. 1. For further details, see [3]. Note that the control-oriented model is designed to capture only those properties of the underwater snake robot dynamics that are relevant for analysis and control design, and it is thus derived for control design and stability analysis purposes [3].

The state vector of the model is chosen as

$$\mathbf{x} = \left[\phi^T, \theta, p_x, p_y, \mathbf{v}_\phi^T, \upsilon_\theta, \upsilon_t, \upsilon_n\right]^T \in \mathbb{R}^{2N+4}, \tag{1}$$

TABLE I: Definition of mathematical terms

Symbol	Description
N	The number of links
l	The length of a link
m	Mass of each link
ϕ_i	Normal direction distance between links i and $i+1$
$\upsilon_{\phi,i}$	Relative velocity between links i and $i+1$
θ	Orientation of the underwater snake robot
υ_θ	Angular velocity of the underwater snake robot
(t_i, n_i)	Coordinates of the CM of link i in the $t-n$ frame
(p_t, p_n)	Coordinates of the CM of the robot in the $t-n$ frame
(p_x, p_y)	Coordinates of the CM of the robot in the global frame
(υ_t, υ_n)	Forward and normal direction velocity of the robot
u_i	Actuator force at joint i
$(f_{x,i}, f_{y,i})$	Fluid force on link i in the global frame
$(f_{t,i}, f_{n,i})$	Fluid force on link i in the $t-n$ frame

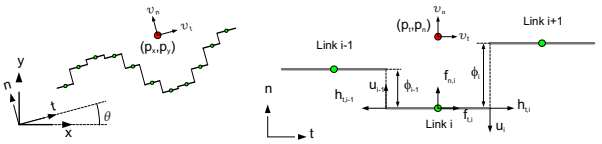

(a) Control-oriented model (b) Kinematics and dynamics of the robot

Fig. 1: Underwater snake robot

where $\phi \in \mathbb{R}^{N-1}$ are the joint coordinates, $\theta \in \mathbb{R}$ is the absolute orientation, $(p_x, p_y) \in \mathbb{R}^2$ is position of CM in the the global frame and $\mathbf{v}_\phi = \dot{\phi} \in \mathbb{R}^{N-1}$ are the joint velocities. $\upsilon_\theta = \dot{\theta} \in \mathbb{R}$ denotes the angular velocity, and $(\upsilon_t, \upsilon_n) \in \mathbb{R}^2$ are the tangential and normal direction velocities of the robot. The complete control-oriented model of the underwater snake robot is given by

$$\dot{\phi} = \mathbf{v}_\phi \tag{2a}$$
$$\dot{\theta} = \upsilon_\theta \tag{2b}$$
$$\dot{p}_x = \upsilon_t \cos\theta - \upsilon_n \sin\theta \tag{2c}$$
$$\dot{p}_y = \upsilon_t \sin\theta + \upsilon_n \cos\theta \tag{2d}$$
$$\dot{\mathbf{v}}_\phi = (-c_n N \mathbf{v}_\phi + N(k_1 \mathbf{A}\mathbf{D}^T \dot{\upsilon}_t/2 + c_p \mathbf{A}\mathbf{D}^T \upsilon_t)\phi + N\mathbf{D}\mathbf{D}^T \mathbf{u})/k_2 \tag{2e}$$
$$\dot{\upsilon}_\theta = -\lambda_1 \upsilon_\theta/(1+\lambda_3) + \lambda_2 \upsilon_t \bar{\mathbf{e}}^T \phi/((N-1)(1+\lambda_3)) \tag{2f}$$
$$\dot{\upsilon}_t = k_3\left(k_1 2c_p(\bar{\mathbf{e}}^T\phi)^2 - k_2 c_t N\right)\upsilon_t + k_3\left(k_2 2c_p \bar{\mathbf{e}}^T\phi - k_1 c_n N \bar{\mathbf{e}}^T\phi\right)\upsilon_n - k_3(k_2 k_1 \phi^T \mathbf{A}\bar{\mathbf{D}}\dot{\mathbf{v}}_\phi/2 + k_2 c_p \phi^T \mathbf{A}\bar{\mathbf{D}}\mathbf{v}_\phi) \tag{2g}$$
$$\dot{\upsilon}_n = k_3\left(Nm2c_p\bar{\mathbf{e}}^T\phi - k_1 c_t N\bar{\mathbf{e}}^T\phi\right)\upsilon_t + k_3\left(k_1 2c_p(\bar{\mathbf{e}}^T\phi)^2 - N^2 m c_n\right)\upsilon_n - \bar{\mathbf{e}}^T\phi k_3(k_1 c_p \phi^T \mathbf{A}\bar{\mathbf{D}}\mathbf{v}_\phi + {k_1}^2 \phi^T \mathbf{A}\bar{\mathbf{D}}\dot{\mathbf{v}}_\phi/2) \tag{2h}$$

where $\mathbf{u} \in \mathbb{R}^{N-1}$ are the transformed actuator forces and

$$\mathbf{A} = \begin{bmatrix} 1 & 1 & & \\ & \ddots & \ddots & \\ & & 1 & 1 \end{bmatrix}, \mathbf{D} = \begin{bmatrix} 1 & -1 & & \\ & \ddots & \ddots & \\ & & 1 & -1 \end{bmatrix},$$
$$\mathbf{e} = \begin{bmatrix} 1 & \dots & 1 \end{bmatrix}^T \in \mathbb{R}^N, \bar{\mathbf{e}} = \begin{bmatrix} 1 & \dots & 1 \end{bmatrix}^T \in \mathbb{R}^{N-1},$$
$$\bar{\mathbf{D}} = \mathbf{D}^T\left(\mathbf{D}\mathbf{D}^T\right)^{-1} \in \mathbb{R}^{N\times N-1},$$

where $\mathbf{A}, \mathbf{D} \in \mathbb{R}^{(N-1)\times N}$, $k_1 = \mu_n/l$, $k_2 = Nm + N\mu_n$ and $k_3 = 1/(Nmk_2 - (k_1\bar{\mathbf{e}}^T\phi)^2)$. The parameters c_t, c_n are the fluid force coefficients due to the drag effect in x and y direction of motion, while μ_n denotes the fluid coefficient

due to the added mass effect in y direction. The parameter $c_p = (c_n - c_t)/2l$ is a propulsion coefficient which maps the normal direction link velocities and the joint coordinates into propulsive fluid forces in the forward direction of locomotion of the underwater snake robot. The coefficient λ_1 determines the drag torque, λ_2 is a constant parameter which gives the scaling of the mapping from average coordinate and forward velocity to rotational acceleration, and λ_3 indicates the torque coefficient due to the added mass effect. For more detail, see [3]. In this paper we choose the transformed actuator forces at the joints according to the linearizing control law

$$\mathbf{u} = \frac{k_2}{N}(\mathbf{D}\mathbf{D}^T)^{-1}(\bar{\mathbf{u}} + \frac{c_n N}{k_2}\dot{\phi} - \frac{N}{k_2}(\frac{k_1}{2}\mathbf{A}\mathbf{D}^T \upsilon_t + c_p \mathbf{A}\mathbf{D}^T \upsilon_t)\phi), \quad (3)$$

where $\bar{\mathbf{u}} \in \mathbb{R}^{N-1}$ denotes the new control inputs. It is easily verifiable that the feedback linearizing control law transforms the joint dynamics (2e) into

$$\dot{\mathbf{v}}_\phi = \bar{\mathbf{u}} \quad (3e^*)$$

III. CONTROLLER DESIGN

The objective of the control design is to make the underwater snake robot track a sinusoidal motion pattern, which consists of horizontal waves that are propagated backwards along the robot from the head to tail. Previous studies in swimming snake robots have been focused on two motion patterns, lateral undulation and eel-like motion. Lateral undulation [1], which is the fastest and the most common form of ground snake locomotion, can be achieved by creating continuous body waves, with no varying amplitude, that are propagated backwards from head to tail. In order to achieve lateral undulation, the snake is commanded to follow the serpenoid curve as proposed in [13]. Eel-like motion can be achieved by propagating lateral axial undulations with increasing amplitude from nose to tail [14].

In this study a general sinusoidal motion pattern is introduced, which can be used for a broad class of motion patterns including lateral undulation and eel-like motion. In particular, the motion pattern is achieved by making each joint $i \in \{1, \cdots, N-1\}$ of the underwater snake robot track the sinusoidal reference signal

$$\phi_{i,\text{ref}}(t) = \alpha \text{g}(i,N)\sin(\omega t + (i-1)\delta) + \phi_0, \quad (4)$$

where α and ω are the maximum amplitude and frequency, respectively, of the sinusoidal joint motion, δ determines the phase shift between the joints, while the function $\text{g}(i,N)$ is a scaling function for the amplitude of joint i which allows (4) to describe a quite general class of sinusoidal functions and corresponding snake motion patterns. For instance, $\text{g}(i,N) = 1$ gives lateral undulation, while $\text{g}(i,N) = (N-i)/(N+1)$ gives eel-like motion [2]. The parameter ϕ_0 is a joint offset coordinate that can be used to control the direction of the locomotion [1], [15]. In particular in [1] and [15], ϕ_0 is seen to affect the direction locomotion in the case of land-based snake robots and fish robots, respectively. Assuming that ϕ_0 is a constant offset, we have

$$\dot{\phi}_{i,\text{ref}} = \alpha \text{g}(i,N)\omega\cos(\omega t + (i-1)\delta), \quad (5)$$

$$\ddot{\phi}_{i,\text{ref}} = -\alpha \text{g}(i,N)\omega^2\sin(\omega t + (i-1)\delta). \quad (6)$$

The control input $\bar{\mathbf{u}}$ is chosen as

$$\bar{\mathbf{u}} = \ddot{\phi}_{\text{ref}} + k_d(\dot{\phi}_{\text{ref}} - \dot{\phi}) + k_p(\phi_{\text{ref}} - \phi), \quad (7)$$

where k_p and k_d are positive scalar controller gains and $\phi_{\text{ref}} \in \mathbb{R}^{N-1}$ are joint reference coordinates. The error dynamics of the joints is therefore given by (2a), (3e*) and (7) as

$$(\ddot{\phi}_{\text{ref}} - \ddot{\phi}) + k_d(\dot{\phi}_{\text{ref}} - \dot{\phi}) + k_p(\phi_{\text{ref}} - \phi) = 0, \quad (8)$$

which is uniformly globally exponentially stable [6]. Note that (8) represents the external dynamics of the underactuated system (2), (7) [16]. The internal dynamics remains to be analysed, and we will consider the velocity dynamics in the next section.

IV. VELOCITY DYNAMICS OF UNDERWATER SNAKE ROBOTS BASED ON AVERAGING THEORY

In this section, averaging theory is applied in order to derive the averaged velocity dynamics of the underwater snake robot in the general case of sinusoidal motion patterns described by (4).

A. Model of the velocity dynamics

We will now derive the averaged velocity dynamics of the underwater snake robot during the general motion pattern described in (4). We assume in the following analysis that ϕ, υ_ϕ and $\dot{\upsilon}_\phi$ are given by (4), (5) and (6). Choosing the state vector $\upsilon = (\upsilon_t, \upsilon_n, \upsilon_\theta) \in \mathbb{R}^3$ and taking into account (4), (5), (6), the velocity dynamics can be written as

$$\dot{\upsilon} = \begin{bmatrix} \dot{\upsilon}_t & \dot{\upsilon}_n & \dot{\upsilon}_\theta \end{bmatrix}^T = \mathbf{f}(t,\upsilon), \quad (9)$$

where

$$\mathbf{f}(t,\upsilon) = \begin{bmatrix} k_3\left(k_1 2c_p f_1(\omega t))^2 - k_2 c_t N\right)\upsilon_t + k_3 f_1(\omega t)(k_2 2c_p \\ k_1 c_n N)\upsilon_n - k_3(k_2 k_1 f_3(\omega t)/2 + k_2 c_p f_2(\omega t)) \\ k_3 f_1(\omega t)\left(Nm2c_p - k_1 c_t N\right)\upsilon_t + k_3(k_1 2c_p(f_1(\omega t))^2 - \\ N^2 m c_n)\upsilon_n - k_3 f_1(\omega t)(k_1 c_p f_2(\omega t) + {k_1}^2 f_3(\omega t)/2) \\ -\lambda_1 \upsilon_\theta/(1+\lambda_3) + \lambda_2 \upsilon_t f_1(\omega t)/((N-1)(1+\lambda_3)) \end{bmatrix}, \quad (10)$$

$$f_1(\omega t) = (N-1)\phi_0 + \sum_{i=1}^{N-1} \alpha \text{g}(i,N)\sin(\omega t + (i-1)\delta), \quad (11)$$

$$\begin{aligned} f_2(\omega t) = &\sum_{i=1}^{N-1}\sum_{j=1}^{N-1}(\frac{k_{\alpha\omega}}{\alpha}\phi_0 a_{ij}\text{g}(j,N)\cos(\omega t + (j-1)\delta) \\ &+ k_{\alpha\omega} a_{ij}\text{g}(i,N)\sin(\omega t + (i-1)\delta)\text{g}(j,N)\cos(\omega t + (j-1)\delta)), \end{aligned} \quad (12)$$

$$\begin{aligned} f_3(\omega t) = &-\sum_{i=1}^{N-1}\sum_{j=1}^{N-1}(\frac{k_{\alpha\omega}^2}{\alpha^3}\phi_0 a_{ij}\text{g}(j,N)\sin(\omega t + (j-1)\delta) \\ &+ \frac{k_{\alpha\omega}^2}{\alpha^2} a_{ij}\text{g}(i,N)\sin(\omega t + (i-1)\delta)\text{g}(j,N)\sin(\omega t + (j-1)\delta)), \end{aligned} \quad (13)$$

and a_{ij} denotes the ij element of the matrix $\mathbf{A}\bar{\mathbf{D}}$. Note that in order to be able to write the velocity dynamics in standard form for averaging, we define the parameter $k_{\alpha\omega} = \alpha^2\omega$.

B. Averaged model of the velocity dynamics

As it is shown in [17], averaging theory is applicable to systems that can be written in the form

$$\dot{\mathbf{x}} = \varepsilon \mathbf{f}(t,\mathbf{x}), \quad (14)$$

where ε is a small positive parameter characterizing the magnitude of the perturbations of the systems and $\mathbf{f}(t,\mathbf{x})$ is $T-$periodic, i.e. periodic in time with period T. A system that 'in average' has similar behavior to the original system (14) can be approximated by

$$\dot{\mathbf{x}} = \varepsilon \mathbf{f}_{av}(\mathbf{x}), \quad (15)$$

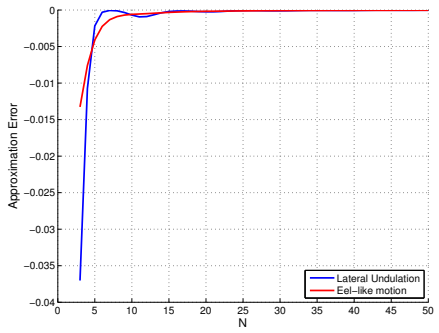

Fig. 2: Approximation Error for parameter k_3

where

$$\mathbf{f}_{av}(\mathbf{x}) = \frac{1}{T}\int_0^T \mathbf{f}(\tau,\mathbf{x})d\tau. \tag{16}$$

We need to rewrite the model of the velocity dynamics of the underwater snake robot (9) in the standard form of averaging (14). To achieve this, we change the time scale from t to $\tau = \omega t$ and define $\varepsilon = 1/\omega$. Furthermore, using the easily verifiable expression $\frac{d}{dt} = \frac{1}{\varepsilon}\frac{d}{d\tau}$, we can express the model (9) in a standard form of averaging, as

$$\frac{d\upsilon}{d\tau} = \varepsilon \mathbf{f}(\tau,\upsilon) \tag{17}$$

where

$$\mathbf{f}(\tau,\upsilon) = \begin{bmatrix} k_3\left(k_1 2c_p f_1(\tau)\right)^2 - k_2 c_t N)\,\upsilon_t + k_3 f_1(\tau)(k_2 2c_p - \\ k_1 c_n N)\upsilon_n - k_3(k_2 k_1 f_3(\tau)/2 + k_2 c_p f_2(\tau)) \\ k_3 f_1(\tau)\,(Nm2c_p - k_1 c_t N)\,\upsilon_t + k_3(k_1 2c_p(f_1(\tau))^2 - \\ N^2 m c_n)\upsilon_n - k_3 f_1(\tau)(k_1 c_p f_2(\tau) + {k_1}^2 f_3(\tau)/2) \\ -\lambda_1 \upsilon_\theta(1+\lambda_3) + \lambda_2 \upsilon_t f_1(\tau)/((N-1)(1+\lambda_3)) \end{bmatrix}. \tag{18}$$

The smallness requirement of ε [17] can always be achieved by choosing $\omega = 1/\varepsilon$ sufficiently large. Now, using (15), we calculate the the averaged model of (17) for general motion pattern locomotion as

$$\frac{d\upsilon}{d\tau} = \varepsilon\frac{1}{2\pi}\int_0^{2\pi} \mathbf{f}(\tau,\upsilon)d\tau. \tag{19}$$

To avoid the complexity of the integral calculation we *Assumption 1*: assume that $Nm(Nm+N\mu_n) \ll (\mu_n \bar{\mathbf{e}}^T \phi/l)^2$. Hence the parameter k_3 is approximated by $k_3 \approx 1/(Nm(Nm+N\mu_n))$.

Remark 1: From Fig. 2 we can see that the approximation error, i.e. $\frac{1}{Nm(Nm+N\mu_n)} - \frac{1}{Nm(Nm+N\mu_n)-(\mu_n\bar{\mathbf{e}}^T\phi/l)^2}$, is small for an underwater snake robot with $m = 0.6597$, $l = 0.14$, added mass coefficient $\mu_n = 0.4$, the parameters of the motion pattern $\alpha = 0.2$ m, $\omega = 120^o/s$, $\delta = 40^o$, $\phi_0 = l/8$ m and N taking values from 3 to 50, for both lateral undulation and eel-like motion. Additionally, it is easily seen that for a robot with $N > 10$ the error is almost zero.

Remark 2: Note that Assumption 1 not only simplifies the integral calculation but also leads us to a solution where the averaged velocity dynamics constitute a good approximation of the original velocity dynamics of the system. If Assumption 1 is disregarded, then the averaged velocity dynamics becomes faster than the original one, i.e. the forcing terms in the averaged model and the original one are different [9]. In this study, using Assumption 1, we show that the classical averaging method can be applied for swimming robots, avoiding to derive the averaged velocity dynamics by scaling the original forcing terms by functions of motion pattern parameters, as it is presented in [9]. This means that the proposed averaged model can be derived using directly the classical averaging, avoiding a control-oriented data-driven averaging approach; a solution presented in [9] for fish robots based on a simulation comparison of the original model and the averaged model obtained through classical averaging.

By taking the trigonometric expansion of the expressions (11)-(13) and choosing the parameters as in (24), the averaged model of the velocity dynamics can be written as

$$\frac{d\upsilon}{d\tau} = \varepsilon(\mathscr{A}\upsilon + \mathbf{b}), \tag{20}$$

where $\mathscr{A}$ and $\mathbf{b}$ are given by (22) and (23), respectively. Since $d/d\tau = \varepsilon d/dt$, by changing the time scale from τ to t, the averaged model can be expressed as

$$\dot{\upsilon} = \mathscr{A}\upsilon + \mathbf{b}. \tag{25}$$

From (25) we see that the averaged model of the velocity dynamics of an underwater snake robot during the sinusoidal motion given by (4) is a linear system and depends on the parameters of the motion pattern, α ω, δ, ϕ_0, the physical parameters of the robot and the parameters of the external forces (i.e. fluid forces and torques).

Remark 3: Note that the averaged model of the velocity dynamics is general in the sense that it comprises a general class of sinusoidal motion patterns given by (4), instead of one specific motion pattern like lateral undulation as in previous works [1], [4]. Hence the proposed averaged model can be used for analysis and control design for a broader class of motion patterns, including lateral undulation and eel-like motion. In addition, the averaged model presented in [1], [4] for lateral undulation of ground snake robots falls out as a special case by setting the fluid coefficients due to the added mass effects to zero (i.e. $\mu_n = 0$ and $\lambda_3 = 0$).

V. STABILITY ANALYSIS OF THE AVERAGED VELOCITY DYNAMICS

In this section we analyse the stability properties of the averaged model (25). Initially, we need to remove the constant offset term $\mathbf{b}$. We do so by employing the coordinate transformation $\mathbf{z} = \upsilon + \mathscr{A}^{-1}\mathbf{b}$, which transforms (25) to

$$\dot{\mathbf{z}} = \dot{\upsilon} = \mathscr{A}(\mathbf{z} - \mathscr{A}^{-1}\mathbf{b} + \mathbf{b}) = \mathscr{A}\mathbf{z}. \tag{26}$$

Using Mathematica, the eigenvalues of $\mathscr{A}$ are found as

$$\begin{aligned} s_1 &= \frac{2c_p l\mu_n(\alpha^2\mu_1 + 2\phi_0^2(N-1)^2) - l^2(c_n m + c_t(m+\mu_n))N^2 - \sqrt{\Delta}}{2l^2 m(m+\mu_n)N^2} \\ s_2 &= \frac{(c_n - c_t)(2\phi_0^2 + \alpha^2\mu_1)\mu_n + 4(c_t - c_n)\phi_0^2\mu_n N}{2l^2 m(m+\mu_n)N^2} \\ &\quad - \frac{((c_n + c_t)l^2 m + (2(c_t - c_n)\phi_0^2 + c_t l^2)\mu_n)N^2 - \sqrt{\Delta}}{2l^2 m(m+\mu_n)N^2} \\ s_3 &= -\lambda_1/(1+\lambda_3) \end{aligned} \tag{27}$$

where $\Delta = l^2(c_n m - c_t(m+\mu_n))^2 N^2(4\phi_0^2(N-1)^2 + l^2N^2)$. In order to show that the equilibrium point $\mathbf{z} = 0$ is globally exponentially stable we need to show that all eigenvalues of $\mathscr{A}$ are in the negative complex half plane [6].

By employing a symbolic inequality solver in Mathematica, with conditions, $m > 0$, $l > 0$, $\mu_n > 0$, $N > 1$, $0 < c_t < c_n$ and $\alpha > 0$, it can be shown that the eigenvalues of the

$$\mathscr{A} = \begin{bmatrix} \frac{\mu_n c_p(2(N-1)^2\phi_0^2+\alpha^2\mu_1)}{Nm(Nm+N\mu_n)l} - \frac{c_t}{m} & (N-1)\phi_0(\frac{2c_p}{Nm} - \frac{\mu_n c_n}{m(Nm+N\mu_n)l}) & 0 \\ (N-1)\phi_0(\frac{2c_p}{Nm+N\mu_n} - \frac{\mu_n c_t}{m(Nm+N\mu_n)l}) & \frac{\mu_n c_p(2(N-1)^2\phi_0^2+\alpha^2\mu_1)}{Nm(Nm+N\mu_n)l} - \frac{Nc_n}{Nm+N\mu_n} & 0 \\ \frac{\lambda_2}{1+\lambda_3}\phi_0 & 0 & \frac{-\lambda_1}{1+\lambda_3} \end{bmatrix} \tag{22}$$

$$\mathbf{b} = \begin{bmatrix} B_1 \\ B_2 \\ 0 \end{bmatrix} = \begin{bmatrix} \frac{\mu_n k_{\alpha\omega}^2 \mu_3}{4Nml\alpha^2} - \frac{c_p k_{\alpha\omega}\mu_2}{2Nm} \\ -\frac{\mu_n c_p k_{\alpha\omega}\phi_0((N-1)\mu_2 - p_1p_3 + p_2p_4)}{2Nm(Nm+N\mu_n)l} + \frac{\mu_n^2 k_{\alpha\omega}^2\phi_0((N-1)\mu_3 + p_1p_4 + p_2p_3)}{2Nm(Nm+N\mu_n)l^2\alpha^2} \\ 0 \end{bmatrix} \tag{23}$$

$$\begin{aligned} &p_1 = \sum_{i=1}^{N-1} \mathrm{g}(i,N)\cos((i-1)\delta), \quad p_2 = \sum_{i=1}^{N-1} \mathrm{g}(i,N)\sin((i-1)\delta), \quad \mu_1 = p_1^2 + p_2^2, \quad p_3 = \sum_{i=1}^{N-1}\sum_{j=1}^{N-1} a_{ij}\mathrm{g}(j,N)\sin((j-1)\delta), \\ &p_4 = \sum_{i=1}^{N-1}\sum_{j=1}^{N-1} a_{ij}\mathrm{g}(j,N)\cos((j-1)\delta), \quad \mu_2 = \sum_{i=1}^{N-1}\sum_{j=1}^{N-1} a_{ij}\mathrm{g}(i,N)\mathrm{g}(j,N)\sin((i-j)\delta), \quad \mu_3 = \sum_{i=1}^{N-1}\sum_{j=1}^{N-1} a_{ij}\mathrm{g}(i,N)\mathrm{g}(j,N)\cos((i-j)\delta) \end{aligned} \tag{24}$$

averaged model are in the left half plane under the following conditions

$$\begin{aligned} &\mu_1 < \frac{l^2N^2((c_n+c_t)m+c_t\mu_n)}{\alpha^2(c_n-c_t)\mu_n} \\ &|\phi_0| < \sqrt{\frac{(c_n+c_t)l^2mN^2 + (\alpha^2(c_t-cn)\mu_1 + c_t l^2N^2)\mu_n}{2(c_n-c_t)(N-1)^2\mu_n}} \\ &\mu_1 + \frac{2\phi_0^2(N-1)^2}{\alpha^2} - \frac{l^2(c_n m + c_t(\mu_n - m))N^3 - \sqrt{\Delta}}{\alpha^2(c_n-c_t)\mu_n N} < 0 \end{aligned} \tag{28}$$

Remark 4: The stability conditions (28) hold for an underwater snake robot influenced by drag forces with anisotropic properties, $c_t < c_n$, and added mass effects, $\mu_n > 0$.

The above results are summarized in the following proposition.

Proposition 1: Given an underwater snake robot described by (2), influenced by drag forces with anisotropic properties, $c_t < c_n$, and added mass effects, $\mu_n > 0$, and with the parameter $k_3 \approx 1/(N^2m(m+\mu_n))$. If the joint coordinates, ϕ, and the joint velocities, υ_ϕ, are given by (4-5), and the frequency ω is sufficiently large, then the averaged model of the velocity dynamics, $\dot{\upsilon} = \mathscr{A}\upsilon + \mathbf{b}$, approximates the original ones (9) with the error being of order $1/\omega$.

Remark 5: From (28), it is seen that the amplitude of the sinusoidal motion pattern is essential in the stability conditions. Note that the stability conditions presented in [4] for a ground snake robot, are independent of the amplitude of the lateral undulation. This provides a new input for the stability analysis of swimming snake robots, where both added mass and linear drag effects are considered.

Under the conditions in (28), the averaged system (25) is exponentially stable. Hence, υ will converge exponentially to $-\mathscr{A}^{-1}\mathbf{b}$, which means that the average velocity will converge exponentially to the steady state velocity

$$\bar{\upsilon} = -\mathscr{A}^{-1}\mathbf{b} = \begin{bmatrix} \bar{\upsilon}_t & \bar{\upsilon}_n & \bar{\upsilon}_\theta \end{bmatrix}^T, \tag{29}$$

which is given analytically by (30) (please see next page). It is easily seen that the resulting steady state velocity of the underwater snake robot depends on the parameters of the system (i.e. m, l, N, μ_n, c_n, c_t, λ_1, λ_2), the joint coordinate offset ϕ_0, and is also function of linear and quadratic terms of the frequency, ω, and the amplitude of the sinusoidal motion pattern, α. Additionally, it is easily verifiable that the steady state velocity of the underwater snake robot with zero joint offset ($\phi_0 = 0$) is given by $\bar{\upsilon}_t = \frac{k_{\alpha\omega}l(m+\mu_n)(\alpha^2(c_t-c_n)\mu_2 + k_{\alpha\omega}\mu_3\mu_n)N}{2\alpha^4(c_n-c_t)\mu_1\mu_n - 4\alpha^2c_t l^2(m+\mu_n)N^2}$, $\bar{\upsilon}_n = 0$ and $\bar{\upsilon}_\theta = 0$.

According to Theorem 10.4 in [6], the averaged model of the velocity dynamics (25) under the conditions (28), for sufficiently small ε (i.e. for sufficiently large ω) will approximate the exact velocity dynamics (9) for all time, with the error being of order ε.

Proposition 2: Given an underwater snake robot described by (2), influenced by drag forces with anisotropic properties, $c_t < c_n$, and added mass effects, $\mu_n > 0$. If Assumption 1 is satisfied, the joint coordinates ϕ are given by (4), (5) and (6), and the conditions (28) are satisfied, then there exist $k > 0$ and $\omega^* > 0$ such that for all $\omega > \omega^*$,

$$\|\upsilon(t) - \upsilon_{\alpha\upsilon}(t)\| \leq k/\omega, \text{ for all } t \in [0,\infty) \tag{31}$$

where $\upsilon(t)$ denotes the exact velocity of the underwater snake robot given by (9) and $\upsilon_{\alpha\upsilon}(t)$ is the average velocity given by (25). Moreover, the average velocity $\upsilon_{\alpha\upsilon}(t)$ of the underwater snake robot will converge exponentially fast to the steady state velocity $\bar{\upsilon}$ given by (30).

Remark 6: Proposition 2 states mathematically that for an underwater snake robot influenced by drag forces with anisotropic properties and added mass effects, forward propulsion is achieved by the general sinusoidal motion pattern given in (4). Furthermore, the results give an analytical expression for the steady state velocity as a function of the motion pattern parameters α, ω, δ, and ϕ_0, i.e. the amplitude, the frequency, phase shift and offset of the joint motion during general sinusoidal motion pattern. Note that the results of this study are general and constitute a powerful tool in order to achieve faster motion by choosing the appropriate motion pattern and the best combination of the gait parameters.

Similar studies are presented for the special case of lateral undulation motion pattern for eel-like robots [7] and ground snake robots [1], [4], and Proposition 2 extends and unifies the results of these studies. In particular, as discussed in the Introduction, earlier studies for ground snake robots [1], [4] and eel-like robots, where the added mass effects and fluid torques are neglected [7], show that the average forward

$$\begin{bmatrix} \bar{v}_t \\ \bar{v}_n \\ \bar{v}_\theta \end{bmatrix} = \begin{bmatrix} \dfrac{k_{\alpha\omega}\left(l^2 m(m+\mu_n)\left(k_{\alpha\omega}\mu_3\mu_n - 2c_p l\mu_2\alpha^2\right)\left(\dfrac{2c_p\mu_n c_1}{lm} - 2c_n N^2\right) - 2\phi_0^2\mu_n(c_n m - c_t(m+\mu_n))(N-1)\left(k_{\alpha\omega}\mu_n c_2 - \alpha^2 2c_p l c_3\right)\right)}{K_1} \\ \dfrac{\phi_0 k_{\alpha\omega}(m+\mu_n)\left(\mu_n\left(\dfrac{2c_p\mu_n c_1}{l(m+\mu_n)N^2} - 2c_t\right)\left(k_{\alpha\omega}\mu_n c_2 - \alpha^2(c_n - c_t)c_3\right) - 2\left((c_t - c_n)\mu_2\alpha^2 + k_{\alpha\omega}\mu_3\mu_n\right)(c_n m - c_t(m+\mu_n))(N-1)\right)}{K_1} \\ \dfrac{\phi_0 k_{\alpha\omega}\lambda_2\left(l^2 m(m+\mu_n)\left(k_{\alpha\omega}\mu_3\mu_n - 2c_p l\mu_2\alpha^2\right)\left(\dfrac{2c_p\mu_n c_1}{lm} - 2c_n N^2\right) - 2\phi_0^2\mu_n(c_n m - c_t(m+\mu_n))(N-1)\left(k_{\alpha\omega}\mu_n c_2 - \alpha^2 2c_p l c_3\right)\right)}{K_1} \end{bmatrix} \tag{30}$$

$$K_1 = 2\alpha^2 l^3\lambda_1 N\left(m(m+\mu_n)\left(\frac{(c_n-c_t)\mu_n c_1}{l^2(m+\mu_n)N^2} - 2c_t\right)\left(\frac{(c_n-c_t)\mu_n c_1}{l^2 m} - 2c_n N^2\right) - \frac{4\phi_0^2(c_n m - c_t(m+\mu_n))^2(N-1)^2}{l^2}\right),$$

$$c_1 = \left(\mu_1\alpha^2 + 2\phi_0^2(N-1)^2\right), \quad c_2 = \mu_3(N-1) + p_2 p_3 + p_1 p_4, \quad c_3 = \mu_2(N-1) - p_1 p_3 + p_2 p_4$$

velocity of the robot is: 1) proportional to the square of the amplitude of the sinusoidal motion pattern, 2) proportional to the gait frequency and 3) depends also on the weighted sum of the constant phase shift between the joints. However, in this paper, it is shown that the average forward velocity of an underwater snake robot, influenced both by added mass and linear drag effects, and under any sinusoidal gait pattern, is: 1) a function of the amplitude of the sinusoidal motion pattern, 2) depends on a linear and a nonlinear terms of the gait frequency and 3) depends on the phase shift between the joints.

VI. SIMULATION RESULTS

This section presents simulation results, for lateral undulation and eel-like motion, to investigate the validity of the derived properties for the averaged velocity dynamics of an underwater snake robot. The exact model of the underwater snake robot is given by (2) under the assumption that ϕ is controlled by (4), while the averaged model of the underwater snake robot is given by (25). Both models are implemented and simulated in Matlab R2011b. The dynamics was calculated using ode45 solver in Matlab with a relative and absolute error tolerance of 10^{-6}.

A. Simulation parameters

We consider an underwater snake robot having $N = 10$ links of length $l = 0.14$ m and mass $m = 0.6597$ kg. Furthermore, we choose the fluid forces and torque coefficients as $c_t = 0.45$, $c_n = 5$, $\mu_n = 0.4$, $\lambda_1 = 0.5$, $\lambda_2 = 20$ and $\lambda_3 = 0.01$, the initial values as ($\phi = 0$, $\theta = 0$, $p_t = 0$, $p_n = 0$, $v_\phi = 0$, $v_\theta = 0$, $v_t = 0$, $v_n = 0$). Note that, as it is shown in [3], for these coefficients the qualitative and quantitative behavior of the control-oriented model of an underwater snake robot (2) is similar to the behavior of the complex model presented in [2]. The fluid forces and torque coefficients of the complex model represent an physical swimming robot. For more detailed explanation please see [2]. The joint reference coordinates were calculated according to the motion pattern (4) with $\alpha = 0.05$ m, $\omega = 120^\text{o}/\text{s}$, $\delta = 40^\text{o}$. The values of the joint offset angle, ϕ_0, will be presented for each simulation result. Furthermore, in order to achieve the desired motion patterns (4) the joint PD controller (7) is used with the controller gains $k_p = 20$ and $k_d = 5$.

B. Simulation results for lateral undulation

The motion of the underwater snake robot during lateral undulation is first simulated with the joint offset angle $\phi_0 = 0$ m, i.e. locomotion along the earth-fixed x axis. For the simulation parameters of the underwater snake robot given in the previous subsection, the eigenvalues of the averaged system, $s_1 = -4.7183$, $s_2 = -0.6821$, $s_3 = -0.4950$, are all in the left half complex plane, which means that the conditions (28) hold for the chosen parameters of the underwater snake robot. In addition, in Fig. 2 it is shown that Assumption 1 holds for the simulated robot. Hence Proposition 2 gives that the average velocity will converge exponentially fast to the steady state velocity given in (30), which for the given parameters is $\bar{v}_t \approx 0.2338$ m/s, $\bar{v}_n = 0$ m/s and $\bar{v}_\theta = 0^\text{o}/\text{s}$. The simulation results are presented in Fig. 3. The top left plot illustrates the global CM position of the underwater snake robot, while the other three plots show the exact and the average velocities of the underwater snake robot. The simulation results shown in Fig. 3 verify that the velocities of the averaged model converge to the expected values of the steady state velocities. Furthermore, the error between the exact velocities and the averaged one of the underwater snake robot are almost zero.

We then performed a simulation to study the averaged velocity dynamics during lateral undulation for the joint offset angle $\phi_0 = l/8$ m, i.e. for lateral undulation along a curve. The eigenvalues of the corresponding averaged model are all negative: $s_1 = -0.4950$, $s_2 = -4.7358$, $s_3 = -0.5987$. By Proposition 2 the average velocity of the underwater snake robot should converge to $\bar{v}_t \approx 0.2646$ m/s, $\bar{v}_n \approx 0.0271$ m/s and $\bar{v}_\theta \approx 0.1852^\text{o}/\text{s}$. This agrees with the simulation results shown in Fig. 4. In addition, from Fig. 4 we can see that the averaged model approximate very well the original model also for the case of a nonzero joint offset angle.

In order to investigate how well the averaged system approximates the original system for lower frequencies, we performed a simulation with frequency $\omega = 30^\text{o}/\text{s}$, and joint offset angle $\phi_0 = l/8$ m. The simulation results are presented in Fig. 5. The averaged model is also here stable, with eigenvalues $s_1 = -0.4950$, $s_2 = -4.7358$, $s_3 = -0.5987$, and the steady state velocities converge to $\bar{v}_t \approx 0.0661$ m/s, $\bar{v}_n \approx 0.0068$ m/s and $\bar{v}_\theta \approx 0.0463^\text{o}/\text{s}$ as predicted by (30). The simulation results show that even though the deviation between the averaged and the original model increases, the averaged model is still able to approximate the original velocity dynamics quite well even in the case when the frequency of the sinusoidal motion is reduced significantly. Note that the eigenvalues of the averaged system did not change by changing the frequency of the sinusoidal motion because the eigenvalues of the system (27) are independent of the parameter ω.

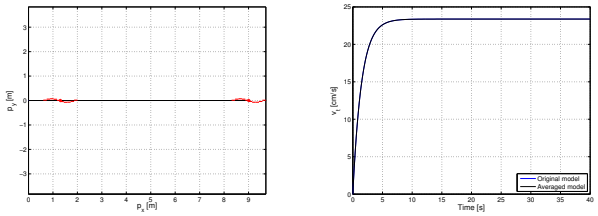

(a) The position of the CM (b) The tangential velocity v_t

(c) The normal velocity v_n (d) The angular velocity v_θ

Fig. 3: Lateral undulation along a straight line ($\phi_0 = 0$ m)

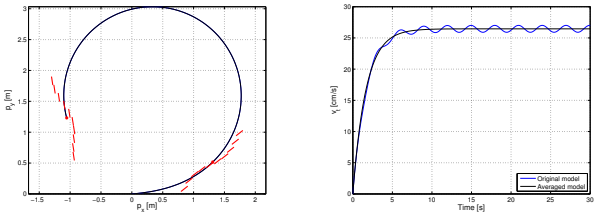

(a) The position of the CM (b) The tangential velocity v_t

(c) The normal velocity v_n (d) The angular velocity v_θ

Fig. 4: Lateral undulation for turning motion with joint offset angle $\phi_0 = l/8$ m and $\omega = 120^o/s$

C. Simulation results for eel-like motion

Eel-like motion is achieved by propagating lateral axial undulations with increasing amplitude from nose to tail. This is achieved by choosing $g(i,N) = (N-i)/(N+1)$ in (4). First, eel-like motion is examined by setting the joint offset angle $\phi_0 = 0$ m. Simulation results are presented in Fig. 6. The eigenvalues of the averaged system, $s_1 = -4.7159$, $s_2 = -0.6798$, $s_3 = -0.4950$, are negative. Thus, by Proposition 2 the average velocity will converge exponentially to the steady state velocity $\bar{v}_t \approx 0.0606$ m/s, $\bar{v}_n = 0$ m/s and $\bar{v}_\theta = 0^o/s$. This is in good accordance with the simulation results shown in Fig. 6. We then chose the joint offset angle $\phi_0 = l/8$ m. The eigenvalues of the corresponding averaged model are then $s_1 = -0.4950$, $s_2 = -4.7334$ and $s_3 = -0.5964$, which shows that the averaged system is also here exponentially stable and by Proposition 2 the average velocity of the underwater snake robot should converge to $\bar{v}_t \approx 0.0686$ m/s,

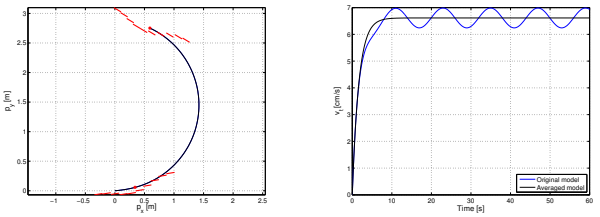

(a) The position of the CM (b) The tangential velocity v_t

(c) The normal velocity v_n (d) The angular velocity v_θ

Fig. 5: Lateral undulation for turning motion with joint offset angle $\phi_0 = l/8$ m and $\omega = 30^o/s$

$\bar{v}_n \approx 0.0070$ m/s and $\bar{v}_\theta \approx 0.0480^o/$ s. This is in good accordance with the simulation results presented in Fig. 7.

Similarly to the lateral undulation case, simulation results during eel-like motion with reduced frequency $\omega = 30^o/s$ and joint offset angle $\phi_0 = l/8$ m are performed. These are presented in Fig. 8. The steady state velocities are expected to converge to $\bar{v}_t \approx 0.0166$ m/s, $\bar{v}_n \approx 0.0017$ m/s and $\bar{v}_\theta \approx 0.0116^o/s$. Note that the averaged model is able to approximate the original velocity dynamics also when reducing the frequency of the eel-like gait pattern (Fig. 8). To conclude, the simulation results for eel-like motion pattern (Fig. 6-8), show that the velocities of the averaged model converge to the expected values of the steady state velocities. A more efficient way for generating the eel-like motion pattern has to be analysed, in the future, in order to reduce the higher oscillation behavior.

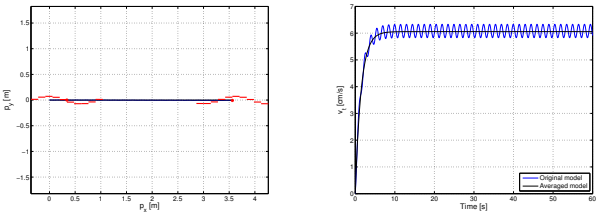

(a) The position of the CM (b) The tangential velocity v_t

(c) The normal velocity v_n (d) The angular velocity v_θ

Fig. 6: Eel-like motion along a straight line ($\phi_0 = 0$ m)

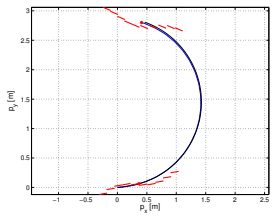

(a) The position of the CM

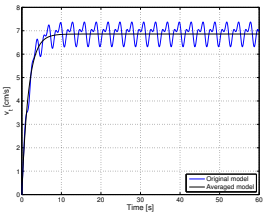

(b) The tangential velocity v_t

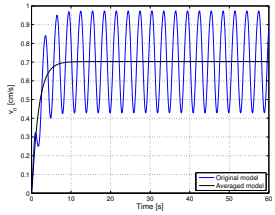

(c) The normal velocity v_n

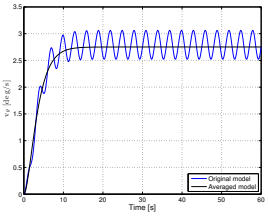

(d) The angular velocity v_θ

Fig. 7: Eel-like motion for turning motion with joint offset angle $\phi_0 = l/8$ m and $\omega = 120^o/s$

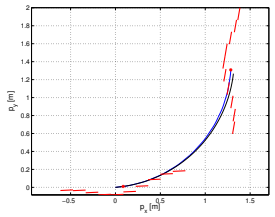

(a) The position of the CM

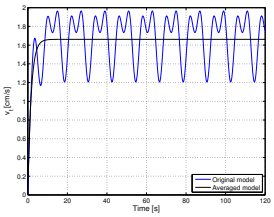

(b) The tangential velocity v_t

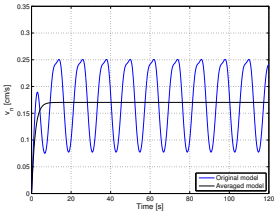

(c) The normal velocity v_n

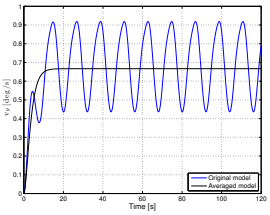

(d) The angular velocity v_θ

Fig. 8: Eel-like motion for turning motion with joint offset angle $\phi_0 = l/8$ m and $\omega = 30^o/s$

VII. CONCLUSIONS AND FUTURE WORK

In this paper, the velocity dynamics of underwater snake robots, during a general sinusoidal gait pattern, was investigated based on averaging theory. It was shown that the average velocity of the underwater snake robot will converge exponentially to a steady state velocity, and an analytical expression for calculating the steady state velocity was derived. An explicit analytical relation was given between the steady state velocity and the amplitude, the frequency, the phase shift and the offset of the joint motion for the case of a sinusoidal gait pattern. In particular, it was shown that the average forward velocity of an underwater snake robot, influenced both by added mass and linear drag effects, and under any sinusoidal gait pattern, is: 1) a function of the amplitude of the sinusoidal motion pattern, 2) depends on a linear and a nonlinear terms of the gait frequency and 3) depends on the phase shift between the joints. The results extend previous results on specific gait patterns and land-based snake robots to a larger class of sinusoidal gait patterns and to underwater snake robots where both linear drag and added mass effects have to be considered. Simulation results were presented both for lateral undulation and eel-like motion. The results of this paper are thus more general and provides a useful tool for achieving faster forward motion by selecting the most appropriate motion pattern and the best combination of the gait parameters. Furthermore, the derived relationship for the averaged velocity dynamics can be used to select the most appropriate motion pattern to achieve the desired velocity requirements, while also taking into account the power consumption requirements. Applying the results of this paper to this end will be a topic of future work.

REFERENCES

[1] P. Liljebäck, K. Y. Pettersen, Ø. Stavdahl, and J. T. Gravdahl, *Snake Robots: Modelling, Mechatronics, and Control*. Springer-Verlag, Advances in Industrial Control, 2013.

[2] E. Kelasidi, K. Y. Pettersen, J. T. Gravdahl, and P. Liljebäck, "Modeling of underwater snake robots," in *Proc. of IEEE Int. Conference on Robotics and Automation*, Hong Kong, China, May 31 - June 7, 2014.

[3] E. Kelasidi, K. Y. Pettersen, and J. T. Gravdahl, "A control-oriented model of underwater snake robots," in *Proc. IEEE International Conference on Robotics and Biomimetics*, Bali, Indonesia, Dec. 5-10 2014, (Submitted). [Online]. Available: https://www.dropbox.com/s/jkea1ddorctmcn7/ROBIO2014.pdf

[4] P. Liljebäck, K. Pettersen, O. Stavdahl, and J. Gravdahl, "Stability analysis of snake robot locomotion based on averaging theory," in *49th IEEE Conference on Decision and Control (CDC)*, Dec 2010, pp. 1977–1984.

[5] P. A. Vela, K. A. Morgansen, and J. W. Burdick, "Underwater locomotion from oscillatory shape deformations," in *Proc. of IEEE Conf. Decision and Control*, vol. 2, Dec. 2002, pp. 2074–2080 vol.2.

[6] H. K. Khalil, *Nonlinear Systems*. 3rd ed. Prentice Hall, New York, 2002.

[7] K. McIsaac and J. Ostrowski, "Motion planning for anguilliform locomotion," *IEEE Transactions on Robotics and Automation*, vol. 19, no. 4, pp. 637–625, 2003.

[8] K. Morgansen, B. Triplett, and D. Klein, "Geometric methods for modeling and control of free-swimming fin-actuated underwater vehicles," *IEEE Transactions on Robotics*, vol. 23, no. 6, pp. 1184 –1199, Dec. 2007.

[9] J. Wang, S. Chen, and X. Tan, "Control-oriented averaging of tail-actuated robotic fish dynamics," in *Proc. of American Control Conference (ACC)*, 2013, pp. 591–596.

[10] E. Westervelt and J. Grizzle, *Feedback Control of Dynamic Bipedal Robot Locomotion (Control and Automation Series)*. CRC PressINC, 2007.

[11] K. Morgansen, P. Vela, and J. Burdick, "Trajectory stabilization for a planar carangiform robot fish," in *Proc. of IEEE Int. Conference Robotics and Automation*, vol. 1, 2002, pp. 756–762.

[12] S. Chen, J. Wang, and X. Tan, "Target-tracking control design for a robotic fish with caudal fin," in *Proc. of 32nd Chinese Control Conference (CCC)*, July 2013, pp. 844–849.

[13] S. Hirose, *Biologically Inspired Robots: Snake-Like Locomotors and Manipulators*. Oxford: Oxford University Press, 1993.

[14] J. Colgate and K. Lynch, "Mechanics and control of swimming: a review," *IEEE Journal of Oceanic Engineering*, vol. 29, no. 3, pp. 660 – 673, July 2004.

[15] J. Guo, "A waypoint-tracking controller for a biomimetic autonomous underwater vehicle," *Ocean Engineering*, vol. 33, pp. 2369 – 2380, 2006.

[16] A. Isidori, *Nonlinear Control Systems (Communications and Control Engineering)*. Springer: New York, 1995.

[17] J. Sanders, F. Verhulst, and J. Murdock, *Averaging Methods in Nonlinear Dynamical Systems (Applied Mathematical Science)*. Springer, 2007, vol. 59.